Rayleigh-Bénard convection for viscoplastic fluids

Mohamed Darbouli[a], Christel Métivier[a], Albert Magnin[a]

a. *Laboratoire de Rhéologie, 1301 rue de la Piscine, Domaine Universitaire, BP 53, 38041 GRENOBLE CEDEX 9*

Résumé :

Dans cet article, l'influence des propriétés rhéologiques des fluides à seuil sur le développement des instabilités de Rayleigh-Bénard est étudiée. Grâce à une installation expérimentale adaptée et à la mise en oeuvre d'un fluide à seuil modèle, Carbopol 940*, l'apparition d'instabilités thermo-convectives est mise en évidence par mesure de température et flux thermiques ainsi que par visualisation par ombroscopie des écoulements. L'influence de la contrainte seuil est représentée par* $Y = \tau_y/(\rho g\beta \,\Delta T\, d)$*, qui quantifie l'importance de la contrainte seuil sur les forces de flottabilité. L'apparition des instabilités se produit lorsque* $Y_c \approx 0,01$*.*

Abstract :

In this present paper, the influence of rheological properties of yield stress fluids is investigated on the onset of the Rayleigh-Bénard convection. Different concentrations of Carbopol 940 *are used in an experimental setup. The onset of thermoconvection is shown by measuring temperature differences and also by using shadowgraph flow visualization. The influence of the yield stress is shown through the yield number* $Y = \tau_y/(\rho g\beta \,\Delta T\, d)$*, which represents the importance of the yield stress value against the buoyancy forces. The onset of instability occurs when* $Y_c \approx 0.01$*.*

Keywords : Thermoconvective instabilities, yield stress fluids.

1 Introduction

Thermal convection of viscoplastic fluids is frequently encountered in numerous industrial and environmental applications, for instance cosmetics, food processing, oil industry, geophysics (lava mud), biology. In spite of its practical interest, only few studies have considered the Rayleigh-Bénard convection in viscoplastic fluids. A theoretical approach, developed by Zhang et al [1], shows that the yield stress involves that the motionless (conductive) state is always stable with respect to a small perturbation. Direct numerical simulations have been done by [1] and [2]. These articles show that when the convection is initiated, the amplitude perturbation decreases in time and finally the flow stops in a finite time. We propose, in this experimental study, to investigate the influence of the rheological properties of viscoplastic fluids on the onset of thermoconvective instabilities.

2 Rayleigh-Bénard configuration

2.1 Experimental set-up

The Rayleigh-Bénard set-up is shown schematically in Fig. 1. It corresponds to a circular cell of diameter $D = 179$ mm and height $d = 17$ mm, $d = 30$ mm. The bottom wall, a 6 mm thick $CuZn5$ cooper alloy plate is heated by an electrical heater plate, allowing to control the total heat input Q_t. The temperature-controlled upper wall, a 3 mm thick glass, is obtained by using a circulation from a water bath, with an accuracy in uniformity and stability less than 0.2 K. All temperature measurements are done by means of thermocouples type T, characterized by a measurement precision of 0.75%, at any time, with a Keithley multimeter. The side walls are made of 30 mm thick Plexiglas and are rendered adiabatic.

The onset of convection is determined according to the Schmidt-Milverton principle [3]. The temperature difference ΔT between the top and bottom plates is measured at steady state for each value of Q_t by using thermocouples. In the conductive regime Q_t is proportional to ΔT. Once the onset of the natural convection occurs, the heat transfer becomes active, and the slope of the curve ΔT vs. Q_t decreases significantly, from this point the critical temperature difference ΔT_c is obtained. On the other hand, observation of convection is realized by using shadowgraph technique, as represented in the upper part of the Fig. 1. The cell is lighten with a parallel light beam by means of a light source, a mirror and a collimating lens. The same lens converges the transmitted light at a CCD-camera IRIS, used to record the shadowgraphs on video tape at a rate of 25 frames per second. The shadowgraph technique is usually used and is described in [4] and [5].

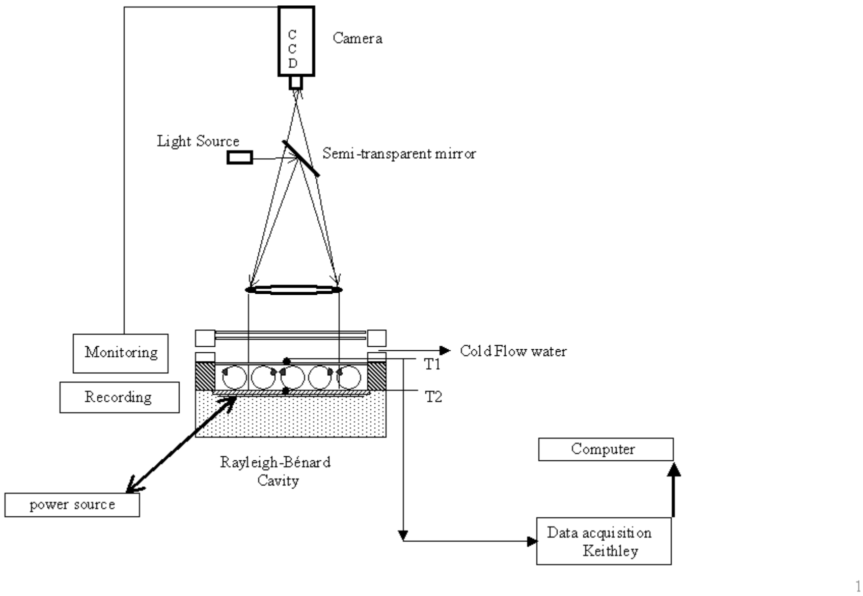

FIG. 1 – Rayleigh-Bénard set-up

2.2 Physical properties of Carbopol 940

The aqueous gels, made from Carbopol polymer (reticulated polyacrylic acid resins), have been used. The polymer is dispersed in distilled water and neutralized with NaOH, see e.g. [6] for further details. The density and thermal properties are essentially the same as for pure water. The rheological properties of the Carbopol gels have been measured using a controlled-stress TA Instrument rheometer (AR-G2) with an angular resolution of 2.5 $\times 10^{-8}$ rad and a torque resolution of 10^{-10} Nm.

The fluid is characterized by a yield stress value τ_y, which depends on the polymer concentration [6]. Rheological properties of five gels are displayed in Fig. 2. Measurements have been done by imposing the shear rate $\dot{\gamma}$ from large to small values. Viscoplastic fluids are usually described by a solid-like phase when the applied stress is smaller than τ_y and a liquid-like phase above. Constitutive law can be read as follows :

$$\tau = \tau_y + \mu_p(\dot{\gamma})\,\dot{\gamma} \quad if \quad \tau > \tau_y \tag{1}$$

$$\dot{\gamma} = 0 \quad if \quad \tau \leq \tau_y, \tag{2}$$

with τ the shear stress, and $\mu_p(\dot{\gamma})$ the plastic viscosity. The plastic viscosity $\mu_p(\dot{\gamma})$ is represented in Fig. 2(b) as a function of $\dot{\gamma}$. As one can observe, a plateau is obtained for low shear rates, above, the fluid presents a shear-thinning behaviour through a decrease in μ_p with $\dot{\gamma}$. The plastic viscosity has been fitted with the modified Carreau-Bird model (dashed lines in Fig. 2(b)) defined by :

$$\mu_p = \mu_0 \left[1 + (\delta\dot{\gamma})^2\right]^{\frac{n-1}{2}} \quad (3)$$

where δ is a curve fitting parameter with dimension of time, μ_0 corresponds to the viscosity at zero shear-rate. One founds in Fig. 2(b), that the modified Carreau-Bird model fits well the results. The mean square relative error is less than 3% for all measurements. The model parameters are given in Table 1 for each gel.

τ_y (Pa)	μ_0 (Pa.s)	δ (s)	n
0.056	43.7	1545.4	0.387
0.045	27.75	1362.8	0.39
0.031	23.08	1461.3	0.423
0.01	3.8	1438	0.54
0.0047	0.19	63.92	0.68

Tab. 1 – Identification of the constitutive law coefficients.

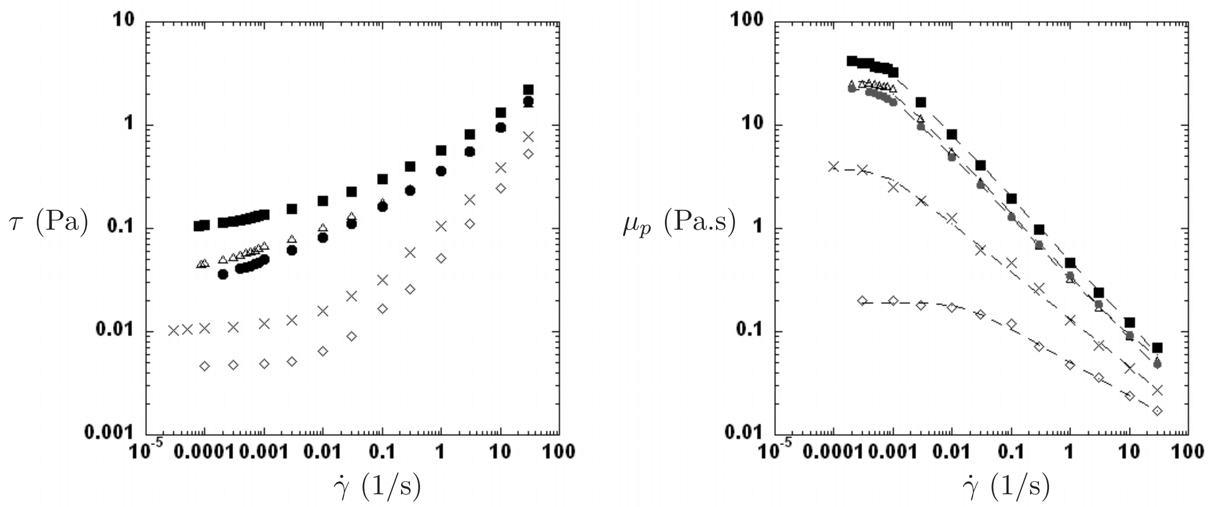

(a) (b)

Fig. 2 – Rheological properties of Carbopol 940 (a) Shear stress as a function of shear rate, (b) Viscosity μ_p as a function of shear rate. (Diamonds : $\tau_y = 0.0047$ Pa, Crosses : $\tau_y = 0.01$ Pa, Black circles : $\tau_y = 0.031$ Pa, Triangles : $\tau_y = 0.045$ Pa, Black squares : $\tau_y = 0.104$ Pa).

In Fig. 2, measurements have been performed by imposing the temperature to $T = 293.15K$. Thermo-dependency of Carbopol gels has been studied in Peixinho [7] by varying temperature from 278.15 to 358.15 K. In this article, the authors show that yield stress does not vary with temperature while μ_p does.

3 Experimental results

3.1 Validation with Newtonian fluid

The RB set-up has been validated first with a Newtonian fluid, distilled water, defined by a viscosity $\mu = 1.3110^{-3}$ Pa.s, a density $\rho = 999.7$ kg.m^{-3}, a thermal diffusivity $\kappa = 1.383810^{-7}$ m^2/s, and a thermal expansion coefficient $\beta = 8.810^{-5}$ K^{-1} at T_m=283.15 K, with T_m is the average of the upper and lower walls temperatures. The transition between the conductive and convective regimes occurs for $\Delta T_c = 0.47$ K, leading to a critical Rayleigh number $Ra_c =$

$1785.73 \pm 1\%$, where Ra is defined by $Ra = \rho g \beta \, \Delta T \, d^3/(\mu\kappa)$. This last result is in good agreement with the theoritical value $Ra_c = 1708$ given in [8], since the relative error is less than 5 %.

3.2 Yield stress fluid results

Concerning the yield stress fluids, experiments have been led with $d = 0.017$ m and $d = 0.03$ m, the results are displayed in Fig. 3(a) and Fig. 3(b) respectively.

One can observe, in Fig. 3, two regimes : the conductive one with a linear behavior of ΔT with respect to Q_t, then a convective regime. It means that instability occurs and critical values ΔT_c can be determined. One notices that for a constant value of d, ΔT_c increases with increasing values of yield stress, which underlines the stabilizing effect of the yield stress.

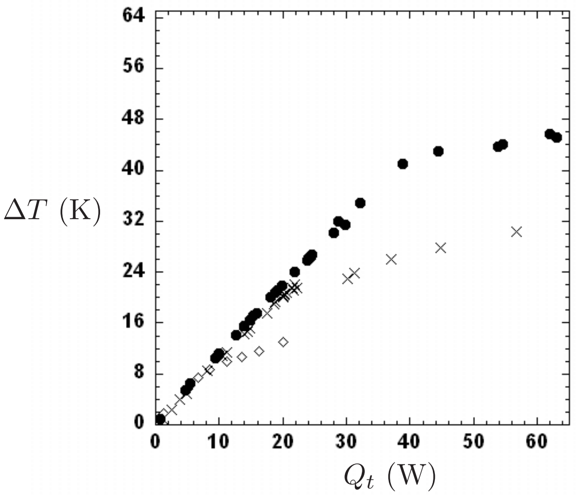

(a) $d = 0.017$ m

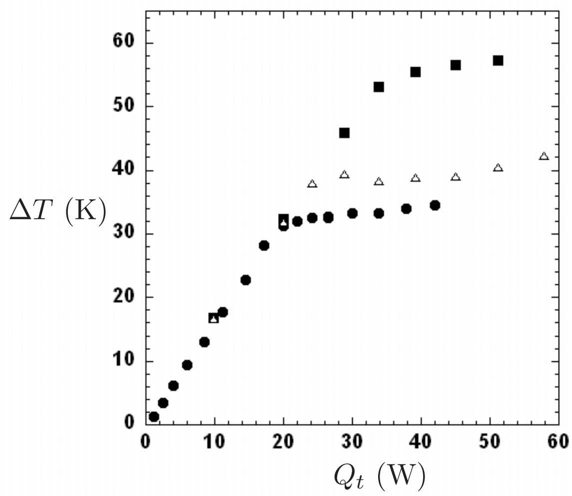

(b) $d = 0.03$ m

FIG. 3 – Temperature difference ΔT as a function of the total heat input Q_t, for different yield stress values of Carbopol 940. (Diamonds : $\tau_y = 0.0047$ Pa, Crosses : $\tau_y = 0.01$ Pa, Black circles : $\tau_y = 0.031$ Pa, Triangles : $\tau_y = 0.045$ Pa, Black squares : $\tau_y = 0.104$ Pa).

Figure 4(a) shows the evolution of the Nusselt number, $Nu = Q_t/Q_{conduction}$ with $Q_{conduction} = S\lambda \, \Delta T/d$, S the area of the lower plate and λ the thermal conductivity, as a function of the Yield number $Y = \tau_y/(\rho g \beta \, \Delta T \, d)$. Y represents the importance of the yield stress against the buoyancy forces. The conductive regime is obtained when $Nu < 1$, corresponding in Fig. 4(a) to $Y > 0.01$. The transition between conduction and convection occurs at $Nu = 1$ and $Y_c \approx 0.01$, for all yield stress values τ_y. Furthermore, when convection increases (or Nu values increase), the yield number remains constant and equal to the critical value Y_c. It means that for $Y_c \approx 0.01$, the buoyancy forces are large enough to balance the yield stress and also to initiate the flow.
The Nusselt number is also displayed in Fig. 4(b) as a function of a generalized Rayleigh number $Ra_g = \rho g \beta \, \Delta T \, d^3/(\mu_0 \kappa + \tau_y d^2)$ which corresponds to the importance of the buoyancy effect against thermal diffusion and shear stress effects. Here, the characteristic scale for viscosity is $\mu_0 + \tau_y d^2/\kappa$. In this sense, the generalized Rayleigh number takes into account both viscous and plastic effects. Figure 4(b) shows that Ra_g increases with increasing Nu in conductive regime. For $Nu \geq 1$, one can notice that $Ra_g \approx 100$, i.e when convection occurs, Ra_g reaches a critical value, then remains constant. Actually, the relation between Ra_g and Y is given by :

$$Ra_g = \frac{1}{(Y + Ra_v^{-1})} \tag{4}$$

where $Ra_v = \rho g \beta \, \Delta T \, d^3/(\mu_0 \kappa)$ corresponds the viscous Rayleigh number. Considering Eq.(4) and our experimental results in Fig. 4(b), one can conclude of the dominant effect of the yield stress, via Y, compared with the viscous effect via Ra_v^{-1}. In this sense Y is the dominant controlled parameter characterizing the influence of plasticity on the onset of convection.

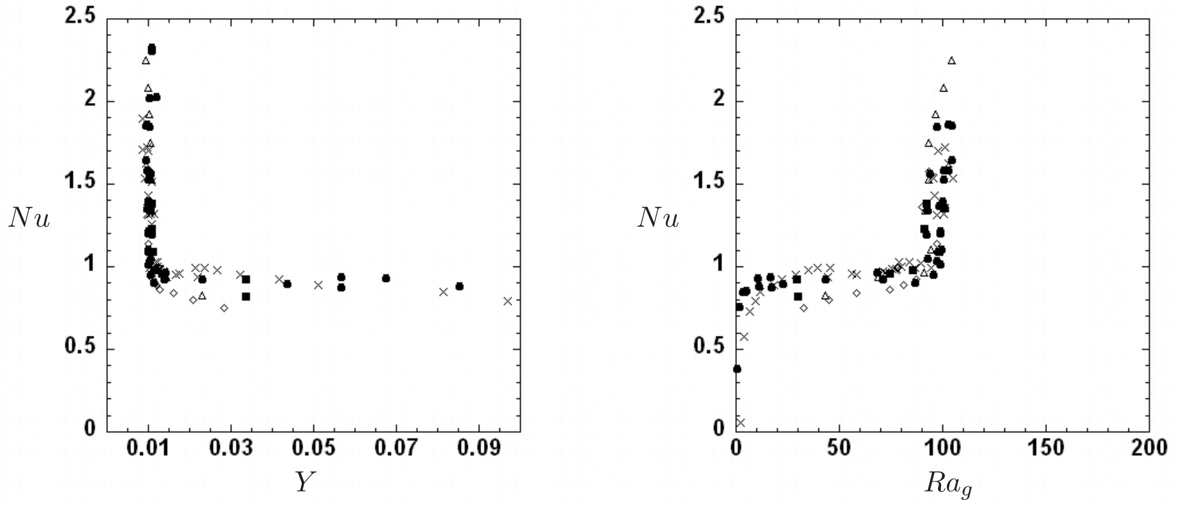

(a) (b)

FIG. 4 – Evolution of Nusselt number as a function of (a) the Yield number Y, (b) the Rayleigh number Ra_g for Carbopol 940. (Diamonds : $\tau_y = 0.0047$ Pa, Crosses : $\tau_y = 0.01$ Pa, Black circles : $\tau_y = 0.031$ Pa, Triangles : $\tau_y = 0.045$ Pa, Black squares : $\tau_y = 0.104$ Pa).

Figure 5 shows the evolution of the flow regimes for different Nu values via shadowgraph snapshots. The reference picture Fig. 5(a) is obtained in the conductive regime since $Nu = 0.94 < 1$. This reference picture has been subtracted to the other ones in order to intensify contrasts. At the beginning of convection $Nu = 1.02$, one can observe motion of fluid through the white and black regions which characterize the boundaries of convective cells. Large values of Nu permit to observe and identify clearly the shape and size of the cells. One finds that rolls are square since the distance between two rolls corresponds to $2d$ (see Fig. 5(c)). This result is similar to the rolls geometry obtained with Newtonian fluids.

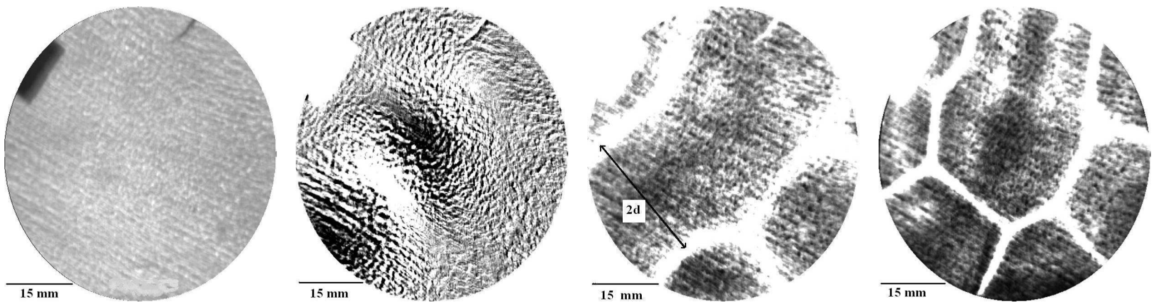

(a) $Nu = 0.94$ (b) $Nu = 1.02$ (c) $Nu = 1.31$ (d) $Nu = 1.72$

FIG. 5 – Shadowgraph visualization for yield stress fluid (Carbopol 940) at different Nu values, $d = 0.017$ m.

4 Conclusion

While theoretical studies [1] show that the Bingham Rayleigh-Bénard configuration remains stable with respect to small perturbations, our experimental results show that convection occurs. Actually, the Bingham model is not a realistic model, especially at the sol-gel transition. This last feature is obviously important to describe the transition between the conductive and convective regimes. The controlled parameter is the Yield number Y and its critical value is $Y_c \approx 0.01$. Our experimental results permit to characterize that Y is the dominant parameter compared with Ra_v^{-1}, the viscous Rayleigh number. Shadowgraph visualizations permit to confirm the onset of instability and also to determine the rolls size. Thermoconvective rolls are found square. In future studies, the influence of the boundary conditions, e.g. slip or no-slip conditions, on the onset of instabilities will be investigated. The influence of the thermo-dependent μ_p on the onset of convection will be also investigated.

Références

[1] Zhang, Vola. D, and Frigaard, I. A., Yield stress effects on Rayleigh Bénard convection, J. Fluid Mech., **566** (2006) 389.

[2] Vikhansky. A, Thermal convection of a viscoplastic liquid with high Rayleigh and Bingham numbers, Phys. Fluids., **21** (2009).

[3] Schmidt R.J., and Milverton S.W., On the instability of a fluid when heated from below, Proc. Roy. Soc. (London)A, **152** (1935)

[4] Merzkirch W., Flow visualisation Academic Press, New York (1974).

[5] Schöpf W., and Patterson J.C., Natural convection in a side-heated cavity : visualization of the initial flow features, J. Fluid Mech., **295** (1995) 357.

[6] Piau J.M., Carbopol gels : Elastoviscoplastic and slippery glasses made of individual swollen sponges Meso- and macroscopic properties, constitutive equations and scaling laws , J.Non-Newtonian Fluid Mech., **144** (2007) 1-29.

[7] Peixinho .J, desaubry .C, and lebouché .M, Heat transfer of a non-Newtonian fluid (Carbopol aqueous solution) in transitional pipe flow, International Journal of Heat and Mass Transfer., **51** (2008) 198-209

[8] Chandrasekhar S., Hydrodynamic and hydromagnetic stability, Oxford : Clarendon press, (1961).